ELSEVIER

International Journal of Mass Spectrometry 179/180 (1998) 195–205

International Journal of Mass Spectrometry

Gas phase agostic bonding in pyridine SiF_n^+ ($n = 1, 3$) cluster ions investigated by the kinetic method

Feng Wang[a], Shuguang Ma[a], Philip Wong[a], R. Graham Cooks[a,*], Fábio C. Gozzo[b], Marcos N. Eberlin[b]

[a]*Department of Chemistry, Purdue University, West Lafayette, IN 47907-1393, USA*
[b]*State University of Campinas, Institute of Chemistry, CP 6154 Campinas, SP 13083-970, Brazil*

Received 1 April 1998; accepted 22 June 1998

Abstract

Loosely bonded cluster ions, $Py_1SiF_3^+Py_2$ and $Py_1SiF^+Py_2$, where Py_1 and Py_2 represent substituted pyridines, are formed by ion/molecule reactions between mass-selected SiF_3^+ or SiF^+ and a mixture of pyridines. The clusters are shown to have loosely bound symmetric structures by MS^3 experiments and ab initio calculations. The SiF_3^+/pyridine dimer is shown to have a trigonal bipyrimidal structure. Relative SiF_3^+ and SiF^+ affinities of the constituent pyridines are measured by the kinetic method, and excellent linear correlations with the proton affinity of meta- and para-substituted pyridines are observed. Gas-phase stereoelectronic parameters (S^k) for SiF_3^+ and SiF^+ are also experimentally measured and show that the binding of the ortho-substituted pyridines is governed by two opposing effects, steric hindrance and agostic bonding. Agostic bonding of the form C–H --- Si^+, is evident in the SiF^+ system, just as it is in the corresponding $SiCl^+$/pyridine dimers. On the other hand, steric hindrance plays a key role in weakening the strength of the interaction of the central SiF_3^+ ion and the ortho-substituted pyridines compared with that in SiF^+-bound cluster ions. The relatively larger Lewis acidity of fluorinated siliconium ions compared with the corresponding chlorinated species shortens the Si–N bond and makes overall steric effects larger in the SiF_n^+ ($n = 1, 3$) systems than in the $SiCl_n^+$ ($n = 1, 3$) systems. The potential application of the kinetic method in recognizing agostic bonding in transition metal systems in the gas phase is also demonstrated in this study. (Int J Mass Spectrom 179/180 (1998) 195–205) © 1998 Elsevier Science B.V.

Keywords: Kinetic method; Agostic bonding; Cluster ions; SiF_3^+, SiF^+, Lewis acidity

Introduction

The study of ion/molecule reactions in the gas phase not only affords the opportunity to investigate the intrinsic reactivities of ions and radicals under solvent- and counterion-free conditions, but also helps provide an understanding of the details of solvation effects. Neutral and charged silicon fluoride species are important intermediates and products in fluorine-based plasma etching of silicon materials for microelectronic devices [1,2]. Gas-phase studies of SiF_n^+ species were initiated historically to add to the understanding of plasma etching processes [3–10] and to characterize the chemical properties of fluorinated siliconium ions, and compare them with the corre-

* Corresponding author.

Dedicated to Professor Fulvio Cacace on his 60th birthday and in recognition of his pioneering and incisive contributions to ion/molecule chemistry.

PII S1387-3806(98)14071-X

sponding carbenium ions [11,12]. Recently, more attention has been paid to the generation and characterization of novel carbenium and siliconium ions with strong Lewis acidity, especially SiF_3^+ [13–18]. In addition, one attempt has been made to increase the reaction efficiency by coordinating the SiF_3^+ to a neutral CO_2 molecule [19].

As a potential ionic Lewis superacid, the reactions of trifluorosilicon cation (SiF_3^+) with *n*-donor bases such as, H_2O, CH_3OH, C_2H_5OH, NH_3 and CH_3NH_2 [15–17], CO [14,18], CO_2 [19], and Xe [13] are of interest. Bond dissociation energies (BDEs) of $SiF_3^+.H_2O$, $SiF_3^+.HF$, $SiF_3^+.CO$, $SiF_3^+.CO_2$ and $SiF_3^+.Xe$ are estimated to be 70 kcal/mol, 46 kcal/mol, 44.1 kcal/mol, 58 kcal/mol, and 35.9 kcal/mol, respectively. In addition, reactions of SiF_3^+ with SiF_4, N_2, $CHCl_3$ and C_2H_4 have been reported [10]. An ordering of SiF_3^+ affinities is given as $F < N_2 < HF < SiF_4 < H_2O$ [10]. On the other hand, few studies have been reported on the reactivity of SiF^+ [3–5,8,15–17]. Because of the combination of $p(\pi)$ back donation and the σ-withdrawing effect of fluorine in SiF_3^+, SiF_3^+ is more reactive than SiF^+ in addition/HF elimination reactions. For example, SiF^+ reacts slowly with H_2O with $k = 7.6 \times 10^{-11}$ cm^3 $molecule^{-1}$ s^{-1} and displays a low efficiency, 0.030, whereas SiF_3^+ has a reaction rate of $k = 1.6 \times 10^{-9}$ cm^3 $molecule^{-1}$ s^{-1} and an efficiency of 0.70 [17]. Those results reflect the fact that the bond strength of Si–F in SiF^+ is stronger than that in SiF_3^+, and this result was also observed in a study of the dissociative scattering of low-energy SiF_3^+ and SiF^+ ions (5–200 eV) from a Cu(100) surface [20]. More recently, accurate heats of formation for SiF_n and SiF_n^+ (n = 1–4) were calculated by using the restricted coupled cluster singles and doubles approach including the effect of connected triples determined using perturbation theory, RCCSD(T) [21]. Bond energies of Si–F in SiF^+, SiF_2^+ and SiF_3^+ are estimated to be 160.0 kcal/mol, 77.5 kcal/mol, and 146.5 kcal/mol, respectively [21].

As a continuation of our interest in thermochemical and structural issues related to cation–ligand bonding [22,23], we report here a study of SiF_3^+ and SiF^+ affinities towards pyridines. The kinetic method is used to order relative affinities toward SiF_3^+ and SiF^+ of alkyl-substituted pyridines. These considerations contribute to one aim of the ongoing study which is to measure BDEs of various cation/pyridine complexes. Ultimately, on the basis of observed linear relationships between cation affinities and the corresponding proton affinities of neutral pyridine ligands, a scale of electrophilicity of cations will be drawn up and forecasts made about their reactivities.

Another aim is to seek information on the nature of bonding in the Lewis acid/base complex, especially auxiliary bonding. Auxiliary bonding, such as hydrogen bonding, agostic bonding, π–π stabilization and salt-bridging [24,25] etc., has been recognized in many chemical systems, including gas-phase ions. The understanding of auxiliary bonding is certainly relevant to the study of enhanced chemical reactivities and conformational changes of neutral molecules induced by cation attachment, especially in peptides and proteins. Therefore, it is very interesting to test whether the kinetic method can be used to explore the form of intramolecular gas-phase auxiliary bonding known as agostic bonding on the basis of analyzing stereoelectronic effects in the SiF_3^+- and SiF^+-bound cluster ions. In agostic bonding a hydrogen atom bridges two heavier elements, often carbon and a metal in a three-center, two-electron bond [26,27].

As an approximate method, the kinetic method has been widely used to determine thermochemical properties through studies of the rates of competitive dissociations of mass-selected weakly bound cluster ions (often cation-bound dimers) undergoing metastable or low energy collision-induced dissociation [22,23]. In comparison with most traditional methods of making thermochemical measurements [28], the kinetic method has the advantage of ready applicability to polar or thermally unstable molecules. In recent years the kinetic method has been extended to address questions of structural identity [29] and to investigate interactions in either cluster ions or charged (i.e. cationized or anionized) monomers [30]. Some of these investigations depend on analyzing the enthalpy and entropy changes associated with cluster ion dissociation [22,23,30,31]. More recently, Cacace has used the kinetic method to obtain the absolute BDEs

of polyatomic cations such as NO^+ [32] and NO_2^+ [33]. Details on the kinetic method are given elsewhere [22,23].

Experimental and theoretical methods

All experiments were performed using a custom-built pentaquadrupole mass spectrometer composed of three mass-analyzing quadrupoles (Q1, Q3, Q5) and two reaction quadrupoles (Q2, Q4) [34]. For tandem mass spectrometry (MS^2) experiments, the SiF_3^+ or SiF^+ ion generated in the ion source was mass-selected by Q1 and was allowed to undergo ion/molecule reactions with a mixture of pyridines in Q2. The reaction products were then analyzed by scanning Q5 with both Q3 and Q4 set in the broad-band transmission (rf-only) mode. To perform MS^3 experiments, the reaction products formed in Q2 were mass-selected using Q3 and subjected to collision-induced dissociation with argon in Q4, whereas Q5 was scanned to record the sequential product ion spectrum [35].

The SiF_3^+ and SiF^+ ions were generated by 70 eV electron ionization of methyl trifluorosilane gas (Crescent Chemical Co., Hauppauge, NY), which was introduced into the ion source via a Granville Phillips leak valve (Granville Phillips Co., Boulder, CO). The nominal sample pressure, typically 5×10^{-6} Torr, was monitored using a single ionization gauge located near Q5. The indicated pressure rose to 4×10^{-5} Torr on addition of the pyridine mixture, and rose to 5×10^{-5} Torr on addition of argon gas to Q4. The collision energy, given by the voltage difference between the ion source and the collision quadrupole, was typically 0 eV (nominal) for ion/molecule reactions and 10 eV for CID. The pyridines (Aldrich Chemical Co., Milwaukee, WI) are commercially available and were used without further purification. The mass-to-charge ratios are reported using the Thomson unit (1 Th = 1 Da/unit charge) [36].

Ab initio calculations were carried out using standard procedures in the GAUSSIAN 94 suite of programs [37]. SiF^+- and SiF_3^+-bound cluster ion geometries were optimized at the Hartree-Fock level of theory by employing the polarization 6-31G(d,p) basis set [38–41]. Improved energies were obtained by incorporating valence electron correlations calculated by second-order Møller-Plesset (MP2) perturbation theory [42], assuming a frozen electron core. Harmonic vibrational frequencies were calculated at the HF/6-31G(d,p) level in order to characterize the stationary points and to obtain the zero-point vibrational energies (ZPVE) for the bond dissociation energy (BDE) calculations. MP2 total energies for the adducts SiF^+/2,6-dimethylpyridine, SiF_3^+/2,6-dimethylpyridine, and the dimeric ions, 2,6-dimethylpyridine/SiF^+/4-methylpyridine and two 2,6-dimethylpyridine/SiF_3^+/4-methylpyridine conformers, are −714.33318, −913.735029, −998.79133, −1197.81878, and −1197.83757 hartree, respectively.

Results and discussion

Like other polyatomic cations [22,23], ion/molecule reactions of SiF^+ with pyridines typically give the following products: (i) protonated monomers, (ii) the mono-SiF^+ adducts and (iii) homo- and hetero-SiF^+- and H^+-bound dimers. In the case of SiF_3^+, some HF loss products from the cationized monomers and dimers are noticeable as well. This result is consistent with the dissociation pattern of SiF_3^+/n-base adducts [15,17], and the relatively higher intensity of electrophilic SiF_3^+-addition/HF loss ions is the result of the weaker Si–F bond dissociation energy (BDE) of SiF_3^+[$D(SiF_2^+–F) = 6.29 \pm 0.10$ eV] compared to that of SiF^+ [$D(SiF^+–F) = 7.04 \pm 0.06$ eV] due to a stabilizing effect in the SiF_2 species associated with an enhancement in the low-energy s orbital character of the lone-pair orbital of the silicon atom [7,43,44]. Furthermore, the overall reaction efficiencies of SiF^+ and SiF_3^+ with pyridines are also consistent with this behavior: although fluorine has a stabilizing effect due to its $p(\pi)$ back donation, it destabilizes SiX_3^+ (X = halogens), a result that is contrary to that found in CX_3^+ ions [12]. Note that the protonated pyridines and the proton-bound dimers are probably formed via charge exchange and subsequent

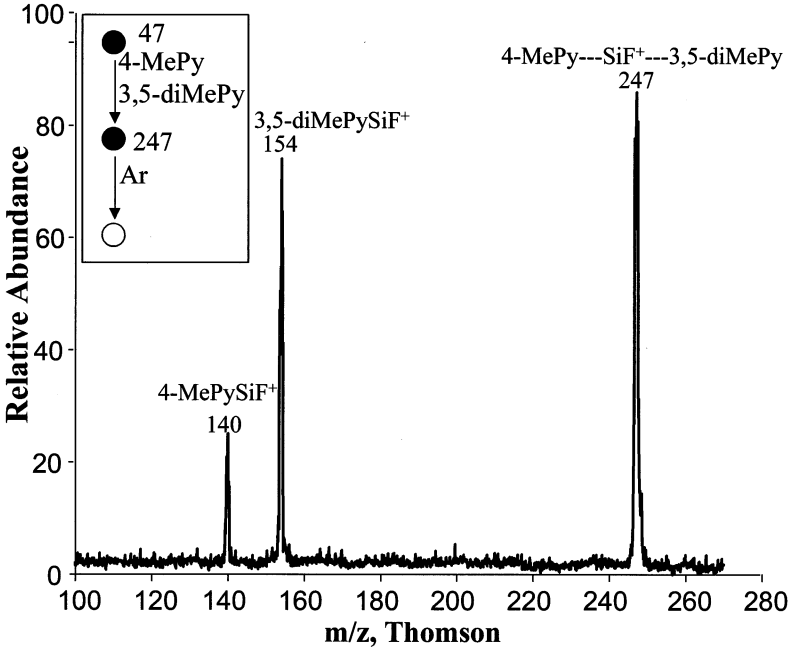

Fig. 1. Sequential product spectrum of mixed dimer 4-methylpyridine/SiF^+/3,5-dimethyl pyridine ion (247 Th).

proton transfer and association reactions, and are not of interest in the present study.

Structures of SiF^+-bound dimeric ions were pursued by using MS^3 experiments. The low-energy CID spectra of the mass-selected dimers show only the SiF^+-cationized monomer in the case of the homodimers and the two component cationized monomers for the mixed dimers. Similar results were observed in the SiF_3^+-bound cluster ions. A typical MS^3 consecutive product spectrum is shown in Fig. 1, taking the dimeric ion 4-methylpyridine/SiF^+/3,5-dimethylpyridine as an example. The ready dissociation of the dimers suggests that the two neutral pyridines are loosely bonded to the central SiF^+ and the dimeric ion is a σ complex ion in which two pyridine ligands are coordinated to the central cation (SiF^+) through the nitrogen atoms.

From the kinetic method, if entropy effects are negligible and reverse activation barriers are zero or constant, the natural logarithm of the relative abundances of the two fragment ions is directly proportional to the difference in the SiF^+ or SiF_3^+ affinities of the two constituent pyridines:

$$\ln \frac{[Py_1SiF_n^+]}{[Py_2SiF_n^+]} = \frac{\Delta(SiF_n^+ \text{affinity})}{RT_{\text{eff}}} \qquad (n = 1, 3) \tag{1}$$

where the terms in brackets of the left-side equation are the product ion abundances, and T_{eff} is the effective temperature of the activated dimer and can be defined as the excess energy above the critical energy per degree of freedom [45]. Due to the lack of independently determined values of SiF_3^+ and SiF^+ affinity, we are only able to measure relative SiF_3^+ and SiF^+ affinities using the kinetic method. If the same electronic effects that influence proton affinities also affect SiF_3^+ and SiF^+ affinities, a linear relationship between the relative proton affinities and the experimental ΔSiF_3^+ or ΔSiF^+ affinities is expected. This is indeed the case as shown in Figs. 2 and 3, and the relative SiF_3^+ and SiF^+ affinities were then calculated with the assumption that T_{eff} is equal to 555 K. This value was used and justified in studies of $SiCl_3^+$ and $SiCl^+$ [46], and Cl^+ [47] affinities towards pyridines and it is also in the range often observed for proton-bound dimers. Note that a $\pm$100 K error of T_{eff}

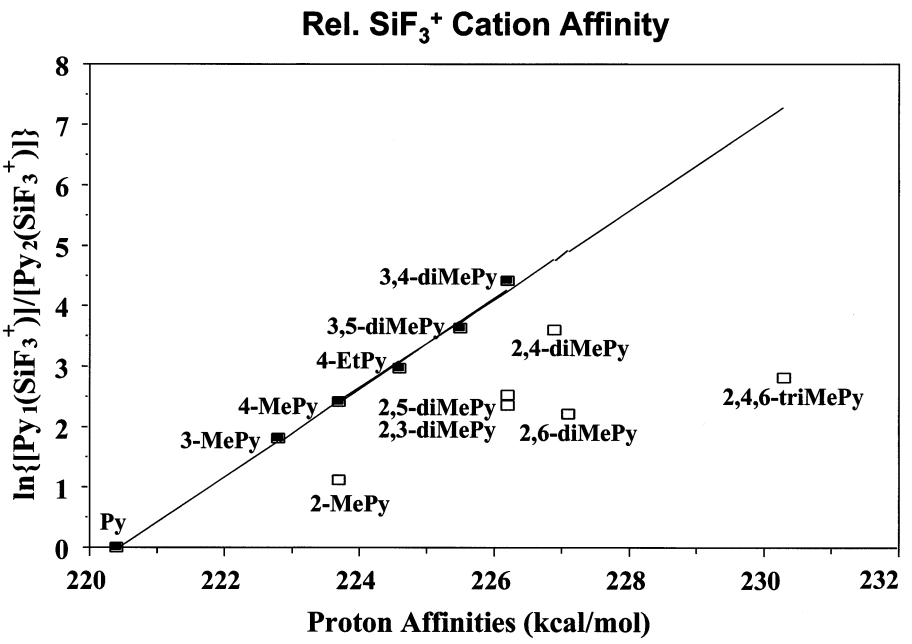

Fig. 2. Linear correlation between $\ln\{[Py_1(SiF_3^+)]/[Py_2(SiF_3^+)]\}$ and proton affinities of component pyridines. Open symbols represent ortho-substituted pyridines that do not correlate.

corresponds to changes in affinities of only ±0.6 kcal/mol. The results are summarized in Table 1. From these data, the relative gas-phase SiF_3^+ and SiF^+ affinities can be ordered as Py < 3-MePy < 4-MePy < 4-EtPy < 3,5-diMePy < 3,4-diMePy. This order is consistent with those for other cations including Cl^+, $OCNCO^+$, $SiCl_3^+$, etc. [46–51], the affinities of which correlate linearly with the proton affinities of meta- and para-substituted pyridines. The relative SiF_3^+ and SiF^+ affinities can then be expressed, in kcal/mol, as given in Eqs. (2) and (3), respectively:

$$\text{Relative } SiF_3^+ \text{ affinities} = 0.74\ PA - 162.3 \quad (2)$$

$$\text{Relative } SiF^+ \text{ affinities} = 0.57\ PA - 125.7 \quad (3)$$

As expected, the correlation of the logarithm of the monomer abundance ratio with proton affinity is generally excellent for meta- and para-substituted pyridines, but poor for the ortho-substituted pyridines. Moreover, for unhindered pyridines the excellent linear relationship between the relative SiF_3^+ and SiF^+ affinities and the corresponding proton affinities, suggests that both SiF_3^+ and SiF^+ form σ complexes (Wheland type adducts) with pyridines. From Table 1, it is also evident that relative SiF_3^+ affinities towards unhindered pyridines are larger than those of SiF^+. This is reflected by the larger coefficient (0.74) relating SiF_3^+ affinities with the corresponding proton affinities [Eq. (2)] in comparison with the value of 0.57 for SiF^+ affinities [Eq. (3)]. This correlation coefficient is dependent on the nature of the ligands and the cation including electronic configuration, size and charge dispersion. The larger coefficient in the case of SiF_3^+ is understandable due to its much stronger Lewis acidity compared to that of SiF^+, which leads to a shorter cation–ligand separation in the adducts. Higher or lower than the expected cation affinities are observed for the ortho-substituted pyridines and are attributed to the combination of steric hindrance and electronic effects between the central cation and the ortho-group(s) of the pyridines. In order to quantify these types of deviations, the gas-phase stereoelectronic parameter (S^k) was introduced and is defined as the deviation from the linear regression line set by the meta- and para-substituted pyri-

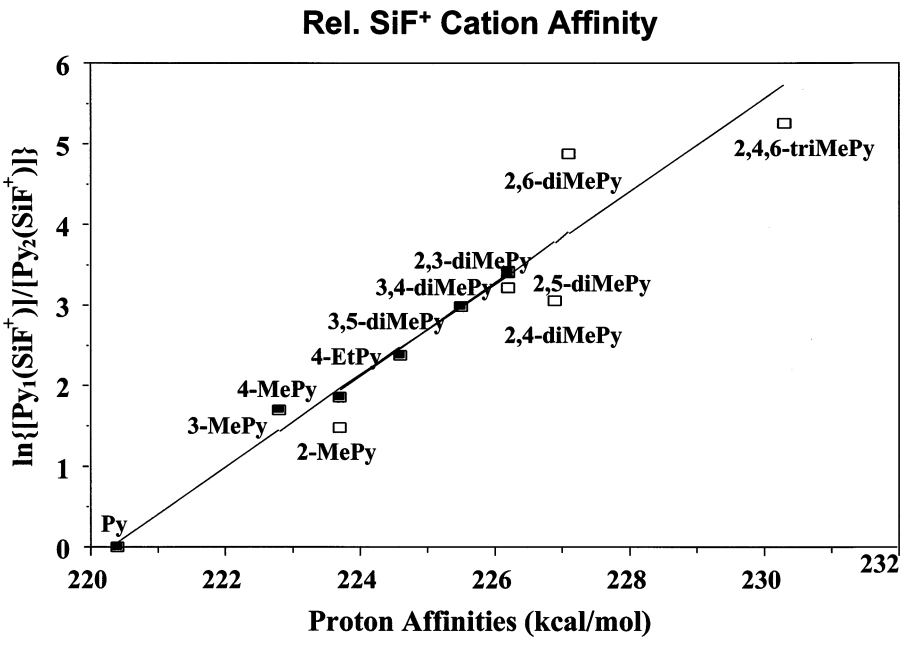

Fig. 3. Linear correlation between $\ln\{[Py_1(SiF^+)]/[Py_2(SiF^+)]\}$ and proton affinities of component pyridines. Open symbols represent ortho-substituted pyridines that do not correlate.

dines [47]. Values of S^k (SiF_3^+) and S^k (SiF^+) are listed along with S^k ($SiCl_3^+$) and S^k ($SiCl^+$) in Table 2. Generally speaking, lower than expected cation affinities for the ortho-substituted pyridines are predicted mainly due to steric hindrance diminishing the interactions of the cations with the neutral ligands: this leads to a negative S^k value. It is evident that S^k (SiF_3^+) values are larger than those of $SiCl_3^+$. Similar results are also observed in the comparison of S^k (SiF^+) vs. S^k ($SiCl^+$), except for 2,3- and 2,6-dimethylpyridine. The relatively larger steric effects in the SiF_n^+ ($n = 1, 3$) system, compared to the corresponding $SiCl_n^+$ ($n = 1, 3$) ions, can be explained by the fact that fluorinated siliconium ions have stronger interaction with Lewis bases than those of chlorinated siliconium ions due to the relatively larger electronegativity and smaller $p(\pi)$ stabilization ability of fluorine atom. Ab initio calculations at the MP2/6-31G(d,p)//HF/6-31G(d,p) level yield BDEs of pyridine adducts of SiF_3^+, $SiCl_3^+$, SiF^+, and $SiCl^+$ as 118.1 kcal/mol, 88.5 kcal/mol, 70.7 kcal/mol, and 65.7 kcal/mol, respectively. This trend in BDEs clearly reflects the order of Lewis acidity of these halogenated siliconium ions which falls in the order $SiF_3^+ > SiCl_3^+ > SiF^+ > SiCl^+$, and also is in good agreement with that of the ionization energies (IEs) of associated neutral radicals SiF_3 (IE = 9.03 ± 0.05 eV) [6,7], $SiCl_3$ (IE = 7.65 ± 0.15 eV) [52], SiF (IE = 7.28 ± 0.2 eV) [6,7] and SiCl (IE = 6.79 ± 0.24 eV) [52]. Furthermore, the larger increase in BDE towards pyridines in going from SiF^+ to SiF_3^+ compared to that seen in going from $SiCl^+$ to $SiCl_3^+$ is mainly due to the fluorine-atom-induced synergistic effect reported in previous studies of fluoro-substituted silyl radicals and anions [53]. Note that chlorinated siliconium ions are more stable than fluorinated ones due to the relatively larger $p(\pi)$ donation from the chlorine atom [12].

The higher than expected SiF^+ affinities towards 2,3- and 2,6-dimethylpyridines, i.e. $S^k_{2,3\text{-diMePy}} = 0.03$ and $S^k_{2,6\text{-diMePy}} = 0.98$, can be explained by the contribution of a form of auxiliary bonding known as agostic bonding [26,27]. Agostic bonding has been explored in many organometallic compounds in

Table 1
Relative SiF_3^+ affinities, SiF^+ affinities, and proton affinities of pyridines

Entry	Pyridines	Py_1:Py_2 [a]	$\ln\{[Py_1(SiF_3^+)]/[Py_2(SiF_3^+)]\}$ [b]	Rel. SiF_3^+ affinity [c]	$\ln\{[Py_1(SiF^+)]/[Py_2(SiF^+)]\}$ [b]	Rel. SiF^+ affinity [c]	Proton affinity/ kcal · mol^{-1} [d]
1	Py		0	0	0	0	220.4
2	3-MePy	2:1	1.82	2.01	1.70	1.87	222.8
3	4-MePy	3:1	2.42	2.67	1.86	2.05	223.7
4	4-EtPy	4:2	2.97	3.28	2.38	2.62	224.6
5	3,5-diMePy	5:3	3.63	4.00	2.99	3.30	225.5
6	3,4-diMePy	6:3	4.42	4.87	3.41	3.76	226.2
7	2-MePy	7:1	1.12	1.24	1.48	1.63	223.7
8	2,3-diMePy	8:3	2.36	2.60	3.42	3.77	226.2
9	2,5-diMePy	9:3	2.53	2.79	3.22	3.55	226.2
10	2,4-diMePy	10:3	3.60	3.97 [f]	3.06	3.37	226.9
11	2,6-diMePy	11:3	2.22	2.45	4.88	5.44	227.1
12	2,4,6-triMePy	12:6	2.82	3.11	5.26	5.80	230.3 [e]

[a] The entry numbers of the pyridines that form the SiF_3^+ and SiF^+-bound dimers used to estimate the SiF_3^+ and SiF^+ affinities.
[b] Experimental results with an average standard deviation of 10% over multiple measurements.
[c] Calculated from Eq. (1) (assuming T_{eff} = 555 K).
[d] Proton affinities are taken from D.H. Aue and M.T. Bowers, in Gas Phase Ion Chemistry, Vol. 2, Academic, New York, 1979. This older set of values is used to facilitate comparison of the present data with those for pyridines bonded to other cations.
[e] Estimated by using the combined inductive and resonance effect of 3.2 kcal/mol for a 4-methyl group and by adding this value to the PA of 2,6-dimethylpyridine. (See [47].)
[f] The larger SiF_3^+ affinity towards 2,4-dimethylpyridine compared to that of other ortho-substituted pyridines is due to the combination of steric hindrance and the resonance effect induced by the para-CH_3 group.

which a typical carbon–hydrogen group interacts with a transition metal center to form a three-center two-electron bond (C–H → M). Agostic bonding in the gas phase was first observed in a study of $SiCl^+$ affinities of a set of alkyl-substituted pyridines [46]. The availability of empty *d*-orbitals on the $SiCl^+$ cation and the sterically favorable orientation of the *o*-methyl group promote intramolecular auxiliary bonding between the hydrogen of the methyl group and the central silicon atom. This auxiliary bonding increases the Si–N bonding strength. More recently, similar phenomena were also reported in studies of PCl_2^+/pyridine adducts [49], $(CH_3O)_2B^+$/pyridine adducts [54] and in protonated P_4 [55]. On the other hand, an alternative explanation of the enhanced SiF^+ affinities to the ortho-substituted pyridine ligands is hydrogen bonding, in the form of C–H(*o*-CH_3) ≡ F(SiF^+). Because higher than expected SiF_3^+ affinities to ortho-substituted pyridines were not observed, we favor the interpretation of the enhancement in SiF^+ affinities is predominantly caused by the agostic bonding effect.

Table 2
Comparison of steric parameters (S^k) for ortho-substituted pyridines

Pyridines	S^k (SiF_3^+) [a]	S^k (SiF^+) [a]	S^k ($SiCl_3^+$) [b]	S^k ($SiCl^+$) [b]
2-MePy	−1.3	−0.48	−0.47	0.15
2,3-diMePy	−1.90	0.03	−0.22	0.55
2,5-diMePy	−1.73	−0.17	−0.32	0.78
2,4-diMePy	−1.18	−0.73	−0.71	−0.17
2,6-diMePy	−2.70	0.98	−0.94	1.62
2,4,6-triMePy	−4.46	−0.47	—	1.44

[a] Obtained from the deviation of experimental data from the regression line. Uncertainties are less than ±0.1.
[b] Taken from [46].

In order to obtain a better understanding of the unexpected increase in SiF^+ affinities towards ortho-substituted pyridines and to compare them with corresponding SiF_3^+ affinities, structures of the adducts SiF^+/2,6-dimethylpyridine, SiF_3^+/2,6-dimethylpyridine and the dimeric ions, 2,6-dimethylpyridine/SiF^+/4-methylpyridine and 2,6-dimethylpyridine/SiF_3^+/4-methylpyridine, were optimized at HF/6-31G(*d*,*p*) level as shown in Figs. 4, 5, and 6. In both the σ complexes formed by SiF^+ or SiF_3^+ with

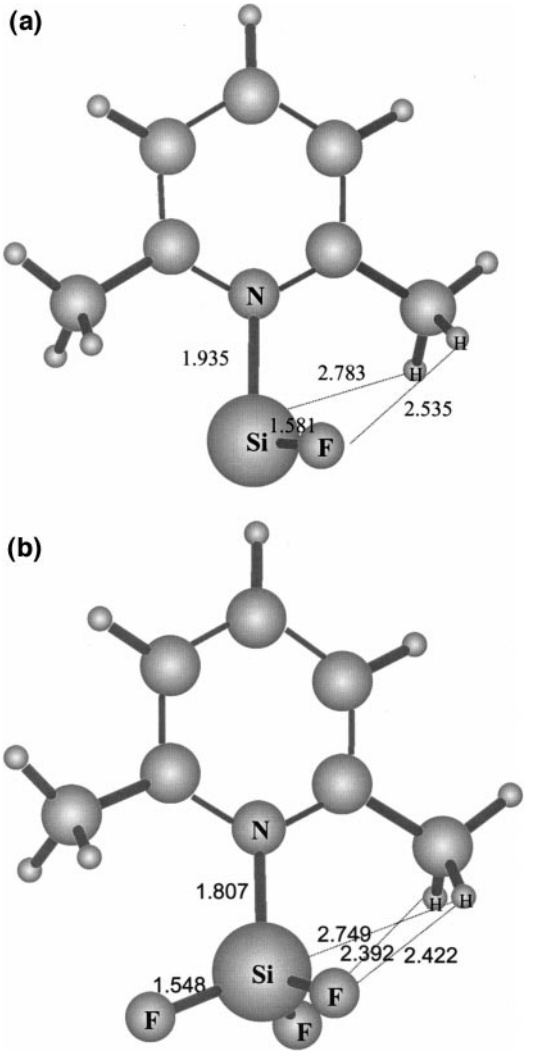

Fig. 4. HF/6-31G(d,p) optimized structures of adducts SiF^+/2,6-dimethylpyridine (a) and SiF_3^+/2,6-dimethylpyridine (b).

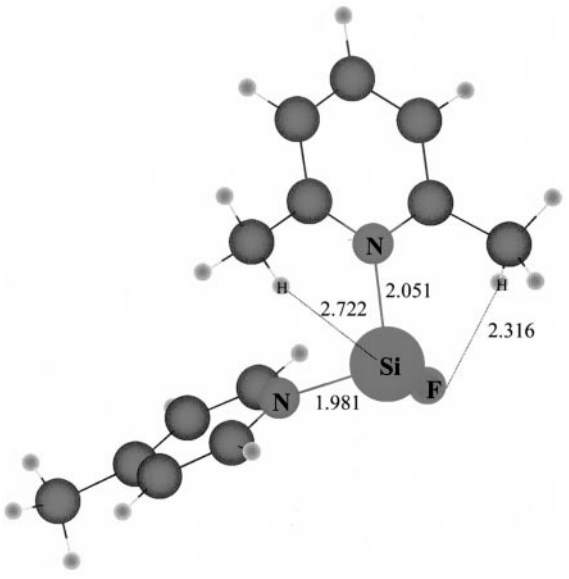

Fig. 5. HF/6-31G(d,p) optimized structure of dimeric ion 2,6-dimethylpyridine/SiF^+/4-methylpyridine.

2,6-dimethylpyridine, the configuration between the central cation and one of the o-CH_3 groups is close to being eclipsed. This is more evident in the adduct SiF_3^+/2,6-dimethylpyridine, which shows that two Si–F bonds interact with two C–H bonds of the o-CH_3 in a "face-to-face" fashion due to a favorable dipole–dipole interaction. As indicated in Fig. 4, in adduct SiF^+/2,6-dimethylpyridine, the shortest distances between Si and F of the SiF^+ group with H(o-CH_3) of 2,6-dimethylpyridine adduct are 2.783 Å and 2.535 Å, respectively, while those in the SiF_3^+/2,6-dimethylpyridine adduct are 2.749 Å and 2.392 Å. Since these distances are all less than the sum of the corresponding atomic van der Waals radii (Si, 2.10 Å; F, 1.47 Å; H, 1.20 Å) [56], the bond strengths of SiF^+ and SiF_3^+ with 2,6-dimethylpyridine are enhanced by agostic and/or hydrogen bonding. As for the structure of the dimeric ion 2,6-dimethylpyridine/SiF^+/4-methylpyridine (Fig. 5), it shows N–Si–F (2,6-dimethylpyridine) and N–Si–F (4-methylpyridine) bond angles of 93.1° and 95.4°, respectively, which are close to the value of 90° expected for the classical trigonal bipyramidal structure as expected. This result suggests that the dimeric ion $Py_1SiF_n^+Py_2$ (n = 1, 3) has a trigonal bipyramidal structure. A similar result is also observed in the structure of the pentacoordinate $SiF_3(CO)_2^+$ [14] and structures of cluster ions formed by $SiCl_3^+$ and $SiCl^+$ with pyridines [46]. Furthermore, two local minimum structures were located in the optimization of the dimeric ion 2,6-dimethylpyridine/SiF_3^+/4-methylpyridine structure (Fig. 6). The trigonal bipyramidal structure [Fig. 6(b)] is estimated to be 11.7 kcal/mol more stable than the structure shown in Fig. 6(a). More importantly, agostic bonding exists only in the SiF^+-bound cluster ion, which leads to a Si

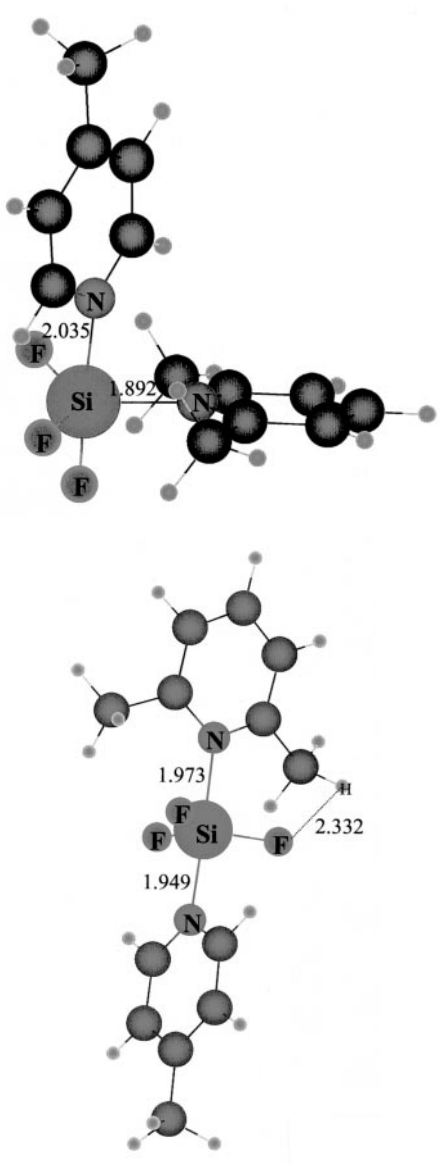

Fig. 6. HF/6-31G(*d*,*p*) optimized structures of dimeric ion 2,6-dimethylpyridine/SiF_3^+/4-methylpyridine.

to H(*o*-CH_3) distance of 2.722 Å, shorter than the sum of their van der Waals radii (3.30 Å) in the dimer. By contrast, note that hydrogen bonding, i.e. C–H (*o*-CH_3)/F, is observed in the calculated structures for SiF^+- and SiF_3^+-bound cluster ions (Figs. 5 and 6). Consequently, the higher than expected SiF^+ affinities towards ortho-substituted pyridines, especially 2,3- and 2,6-dimethylpyridine, must be attributed primarily to the dominant agostic bonding in these cluster ions. This change in binding induced by the second neutral ligand provides another example of solvation effects on intrinsic reactivity of charged species and their role in intracluster reactions [57].

Conclusions

Pentacoordinate Si^+ adducts are formed by reactions of SiF_3^+ and SiF^+ with pyridine mixtures. These adducts have a classical trigonal bipyramidal type of structure with the fluorine atom(s) in the equatorial position(s) and neutral pyridine ligands in the two axial positions. Relative SiF_3^+ and SiF^+ affinities towards meta- and para-substituted pyridines show a similar trend to other polyatomic cations. Affinities towards ortho-substituted pyridines are controlled by two opposing effects, agostic bonding and steric hindrance. Furthermore, enhanced Si^+–N bonding resulting from the agostic contribution, i.e. C–H/Si^+, is more noticeable in SiF^+/pyridine dimers than in SiF_3^+/pyridine dimers while steric hindrance has dominant effects on affinities of SiF_3^+ towards ortho-substituted pyridines. Compared with $SiCl_3^+$ and $SiCl^+$, the overall larger S^k value of SiF_3^+ and SiF^+ towards ortho-substituted pyridines is attributed to the stronger Lewis acidity of the fluorinated siliconium ions compared to that of the chlorinated analogs.

Despite their potential significance, agostic bonding is difficult to characterize in transition metal complexes. Although the presence of C–H → M interactions (M = metal) may often be inferred from a distorted M-alkyl geometry, the true nature of this effect is hard to ascertain. X-ray diffraction, NMR, and vibrational spectroscopies have failed in most cases to detect this interaction [58]. Therefore, the method developed and utilized here is a significant experimental procedure that can be used to locate and explore agostic interactions in the gas phase. Finally, as Cacace has pointed out, studies of “microsolvated” ionic reactions are the most suitable means to understand the details of solvent-reactant interactions that are lost in bulk-phase studies [57]. We expect that the

kinetic method will continue to make contributions to ionic gas-phase supramolecular chemistry.

Acknowledgements

The work at Purdue was financially supported by the National Science Foundation, grant nos. CHE 92-23791 and 97-32670, and the U.S. Department of Energy, Basic Energy Sciences. The research at UNICAMP was supported by the Research Support Foundation of the State of São Paulo (FAPESP) and the Brazilian National Research Council (CNPq).

References

[1] J.W. Coburn, Plasma Etching and Reactive Ion Etching, American Vacuum Society Monograph Series, American Institute of Physics, New York, 1982.
[2] H.F. Winters, J.W. Coburn, Surf. Sci. Rep. 14 (1992) 161.
[3] S.N. Senzer, F.W. Lampe, J. Appl. Phys. 54 (1983) 3524.
[4] B.S. Suresh, J.C. Thompson, J. Chem. Soc. Dalton Trans. (1987) 1123.
[5] E.W. Ignacio, H.B. Schlegel, J. Phys. Chem. 94 (1990) 7439.
[6] B.L. Kickel, E.R. Fisher, P.B. Armentrout, J. Phys. Chem. 97 (1993) 10198 and references therein.
[7] E.R. Fisher, B.L. Kickel, P.B. Armentrout, J. Phys. Chem. 97 (1993) 10204.
[8] R.H. Petrmichl, K.A. Peterson, R.C. Woods, J. Chem. Phys. 89 (1988) 5454.
[9] K. Wang, V. Mckoy, J. Chem. Phys. 97 (1992) 5489.
[10] W.D. Reents, A.M. Mujsce, Int. J. Mass Spectrom. Ion Processes 59 (1984) 65.
[11] M.K. Murphy, J.L. Beauchamp, J. Am. Chem. Soc. 98 (1976) 5781.
[12] G. Frenking, S. Fau, C.M. Marchand, H.F. Grützmacher, J. Am. Chem. Soc. 119 (1997) 6648.
[13] R. Cipollini, F. Grandinetti, J. Chem. Soc., Chem. Commun. (1995) 773.
[14] A.E. Ketvirtis, V.I. Baranov, D.K. Bohme, A.C. Hopkinson, Int. J. Mass Spectrom. Ion Processes 153 (1996) 161.
[15] F. Grandinetti, G. Occhiucci, O. Ursini, G. de Petris, M. Speranza, Int. J. Mass Spectrom. Ion Processes 124 (1993) 21.
[16] M.E. Crestoni, M. Speranza, Int. J. Mass Spectrom. Ion Processes 130 (1994) 143.
[17] A.E. Ketvirtis, V.I. Baranov, A.C. Hopkinson, D.K. Bohme, J. Phys. Chem. A 102 (1998) 1162.
[18] A.E. Ketvirtis, V.I. Baranov, A.C. Hopkinson, D.K. Bohme, J. Phys. Chem. A 101 (1997) 7258 and references therein.
[19] P. Cecchi, M.E. Crestoni, F. Grandinetti, V. Vinciguerra, Angew. Chem. Int. Ed. Engl. 35 (1996) 2522.
[20] H. Yamamoto, Y. Baba, T.A. Sasaki, Appl. Surf. Sci. 101 (1996) 333.
[21] A. Ricca, C.W. Bauschlicher, J. Phys. Chem. A 102 (1998) 876.
[22] R.G. Cooks, J.S. Patrick, T. Kotiaho, S.A. McLuckey, Mass. Spectrom. Rev. 13 (1994) 287.
[23] R.G. Cooks, P. Wong, Acc. Chem. Res. 31 (1998) 379.
[24] S. Campbell, M.T. Rogers, M.E. Martzluff, J.L. Beauchamp, J. Am. Chem. Soc. 117 (1995) 12840.
[25] P.D. Schnier, W.D. Price, R.A. Jockusch, E.R. Williams, J. Am. Chem. Soc. 118 (1996) 7178.
[26] M. Brookhart, M.L.H. Green, J. Organomet. Chem. 250 (1983) 395.
[27] M. Brookhart, M.L.H. Green, L.-L. Wong, Prog. Inorg. Chem. 36 (1988) 1.
[28] M.T. Bowers, Gas Phase Ion Chemistry, Vols. 1–3, Academic: New York, 1979.
[29] P.G. Wenthold, J. Hu, R.R. Squires, J. Am. Chem. Soc. 118 (1996) 11865.
[30] B.A. Cerda, C. Wesdemiotis, J. Am. Chem. Soc. 118 (1996) 11884.
[31] Z. Wu, C. Fenselau, Rapid Commun. Mass Spectrom. 8 (1994) 777.
[32] F. Cacace, G. de Petris, F. Pepi, Proc. Natl. Acad. Sci. USA 94 (1997) 3507.
[33] F. Cacace, G. de Petris, F. Pepi, F. Angelelli, Proc. Natl. Acad. Sci. USA 92 (1995) 8635.
[34] J.C. Schwartz, K.L. Schey, R.G. Cooks, Int. J. Mass Spectrom. Ion Processes 101 (1990) 1.
[35] J.C. Schwartz, A.P. Wade, C.G. Enke, R.G. Cooks, Anal. Chem. 62 (1990) 1809.
[36] R.G. Cooks, A.L. Rockwood, Rapid Commun. Mass Spectrom. 5 (1991) 93.
[37] M.J. Frisch, G.W. Trucks, H.B. Schlegel, P.M.W. Gill, B.G. Johnson, M.A. Robb, J.R. Cheeseman, T. Keith, G.A. Petersson, J.A. Montgomery, K. Raghavachari, M.A. Al-Laham, V.G. Zakrzewski, J.V. Ortiz, J.B. Foresman, J. Cioslowski, B.B. Stefanov, A. Nanayakkara, M. Challacombe, C.Y. Peng, P.Y. Ayala, W. Chen, M.W. Wong, J.L. Andres, E.S. Replogle, R. Gomperts, R.L. Martin, D.J. Fox, J.S. Binky, D.J. Defrees, J, Baker, J.P. Stewart, M. Head-Gordon, C. Gonzalez, J.A. Pople, GAUSSIAN 94, Revision D. 2, Gaussian, Inc., Pittsburgh PA, 1995.
[38] W.J. Hehre, R. Ditchfield, J.A. Pople, J. Chem. Phys. 56 (1972) 2257.
[39] P.C. Hariharan, J.A. Pople, Theor. Chem. Acta 28 (1973) 213.
[40] M.S. Gordon, Chem. Phys. Lett. 76 (1980) 163.
[41] M.J. Frish, J.A. Pople, J.S. Binkley, J. Chem. Phys. 80 (1984) 3265.
[42] C. Møller, M.S. Plesset, Phys. Rev. 46 (1934) 618.
[43] R. Walsh, Acc. Chem. Res. 24 (1981) 246.
[44] R. Walsh, J. Chem. Soc. Faraday Trans. 1, 79 (1983) 2233.
[45] S.L. Craig, M. Zhang, B. Choo, J.I. Brauman, J. Phys. Chem. A 101 (1997) 19.
[46] S.S. Yang, P. Wong, S. Ma, R.G. Cooks, J. Am. Soc. Mass Spectrom. 7 (1996) 198.
[47] M.N. Eberlin, T. Kotiaho, B, Shay, S.S. Yang, R.G. Cooks, J. Am. Chem. Soc. 116 (1994) 2457.

[48] S.S. Yang, G. Chen, S. Ma, R.G. Cooks, F.C. Gozzo, M.N. Eberlin, J. Mass Spectrom. 30 (1995) 807.
[49] S. Ma, P. Wong, R.G. Cooks, F.C. Gozzo, M.N. Eberlin, Int. J. Mass Spectrom. Ion Processes 163 (1997) 89.
[50] P. Wong, S. Ma, S.S. Yang, R.G. Cooks, F.C. Gozzo, M.N. Eberlin, J. Am. Soc. Mass Spectrom. 8 (1997) 68.
[51] P. Wong, S. Ma, F. Wang, R.G. Cooks, J. Organomet. Chem. 539 (1997) 131.
[52] E.R. Fisher, P.B. Armentrout, J. Phys. Chem. 95 (1991) 4765.
[53] C.F. Rodriquez, A.C. Hopkinson, Can. J. Chem. 70 (1992) 2234.
[54] S. Ma, P. Wong, R.G. Cooks, J. Mass Spectrom. 32 (1997) 159.
[55] J.-L. M. Abbout, M. Herreros, R. Notario, M. Esseffar, O. Mó, M. Yáñez, J. Am. Chem. Soc. 118 (1996) 1126.
[56] A. Bondi, J. Phys. Chem. 68 (1964) 441.
[57] F. Cacace, Pure & Appl. Chem. 69 (1997) 227.
[58] G.S. McGrady, A.J. Downs, A. Haaland, W. Scherer, D.C. McKean, Chem. Commun. (1997) 1547.